

**Supplemental materials for
Digitally-assisted structure design of large-size proton exchange
membrane fuel cell**

Wenming Huo^{a,c, ‡}, Linhao Fan^{a,e, ‡}, Yunfei Xu^b, Mohamed Benbouzid^c, Wenzhen Xu^a, Fei Gao^{d,*}, Weizhuo Li^a, Nian Shan^b, Biao Xie^a, Haipeng Huang^b, Bohao Liu^a, Yassine Amirat^f, Chuan Fang^b, Xiaohui Li^b, Quanquan Gan^b, Feiqiang Li^{b,*}, Kui Jiao^{a,e,*}

^a State Key Laboratory of Engines, Tianjin University, Tianjin 300350, China

^b Beijing SinoHytec Co., Ltd., Beijing, 100192, China

^c University of Brest, UMR CNRS 6027 IRDL, 29238 Brest, France

^d Université de Technologie de Belfort-Montbéliard, CNRS, Institut FEMTO-ST,
90000 Belfort, France

^e National Industry-Education Platform for Energy Storage, Tianjin University,
Tianjin 300350, China

^f L@bISEN, ISEN Yncréa Ouest, 29200 Brest, France

Corresponding authors: fei.gao@utbm.fr (Fei Gao), lifeiqiang@autoht.com (Feiqiang Li), kjiao@tju.edu.cn (Kui Jiao)

[‡] The authors have equal contributions

Content

Supplementary Figures	4
Fig. S1	4
Fig. S2	4
Fig. S3	5
Fig. S4	5
Fig. S5	6
Fig. S6	6
Fig. S7	7
Fig. S8	7
Fig. S9	8
Fig. S10	8
Fig. S11	9
Fig. S12	9
Fig. S13	10
Fig. S14	10
Fig. S15	11
Fig. S16	11
Supplementary Tables	12
Table S1.....	12
Table S2.....	13
Table S3.....	14
Table S4.....	15
Table S5.....	16
Table S6.....	17
Table S7.....	18
Table S8.....	19
Table S9.....	20
Table S10.....	21
Table S11.....	22
Table S12.....	23

Supplementary Notes	24
Note S1	24
Note S2	27
Note S3	29
Supplementary Reference.....	32

Supplementary Figures

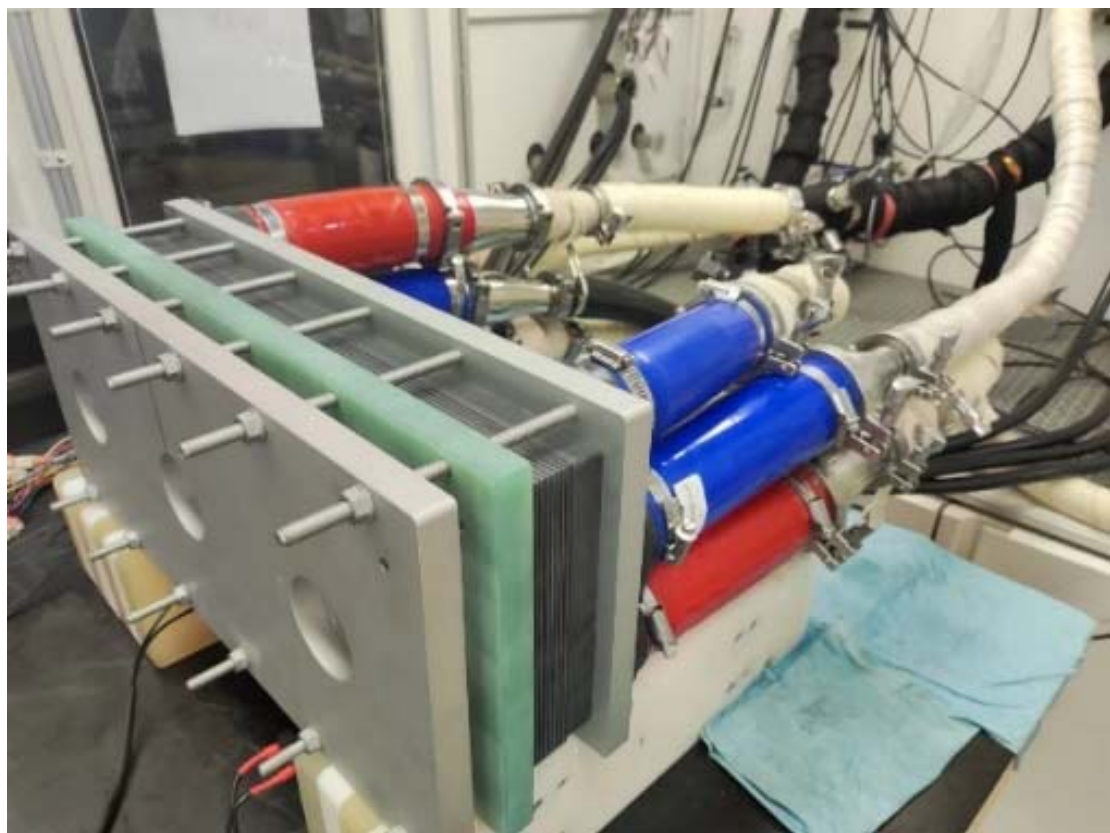


Fig. S1 Fuel cell testing experimental setup.

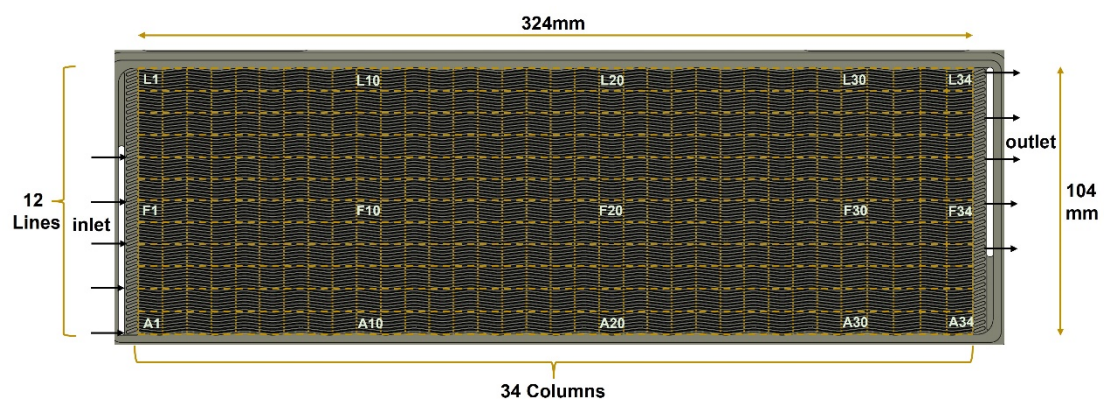


Fig. S2 Segment method and regions.

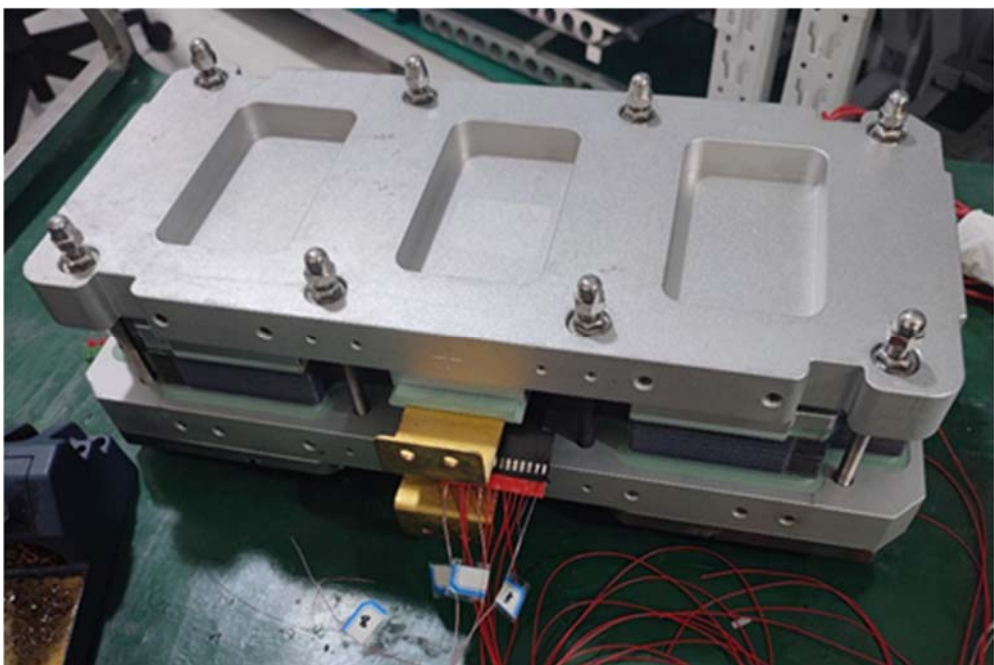


Fig. S3 The assembly of single cell for segmented fuel cell testing.



Fig. S4 Experimental setup for segmented fuel cell testing.

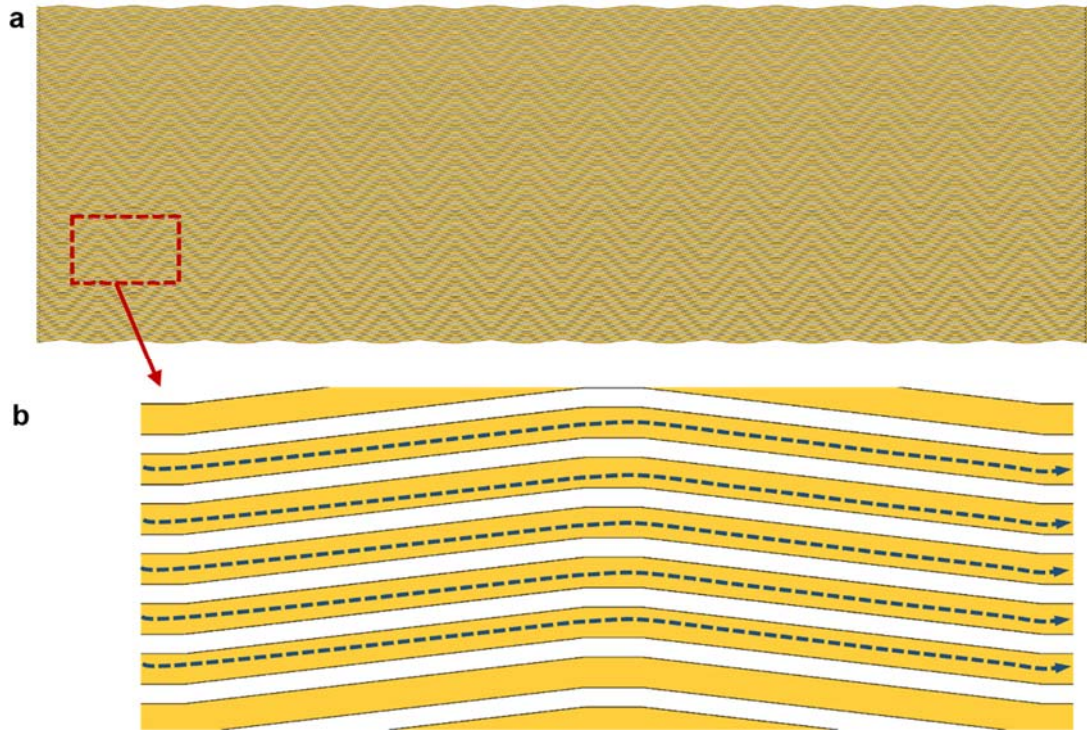


Fig. S5 3D structure of cathode channels. (a) Cathode wavy channels and (b) gas flow direction.

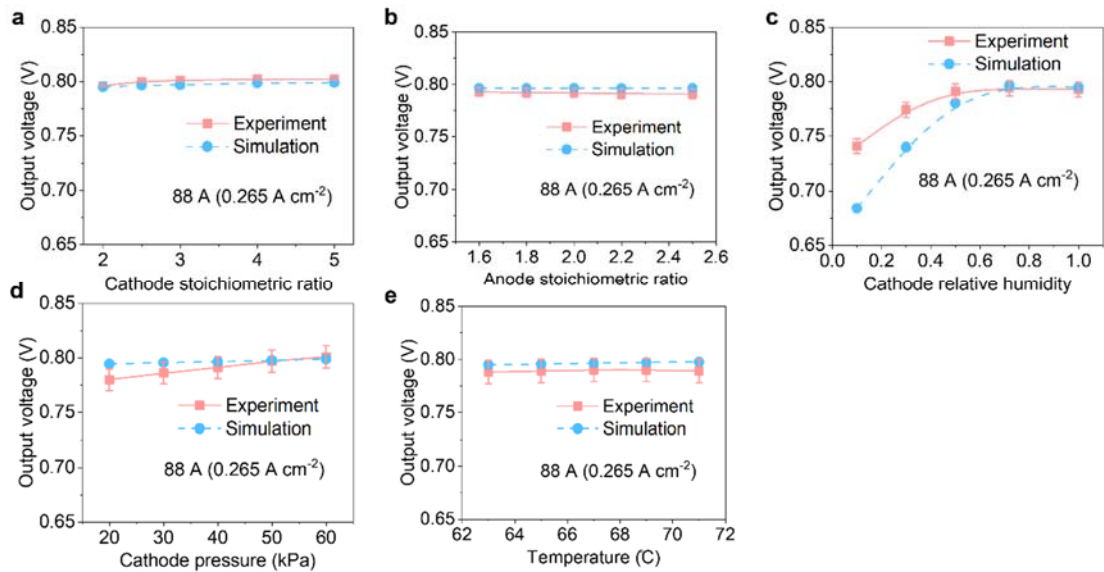


Fig. S6 Simulation performance of five sensitive parameters compared with experimental data at the current density of $88 \text{ A} (0.265 \text{ A cm}^{-2})$.

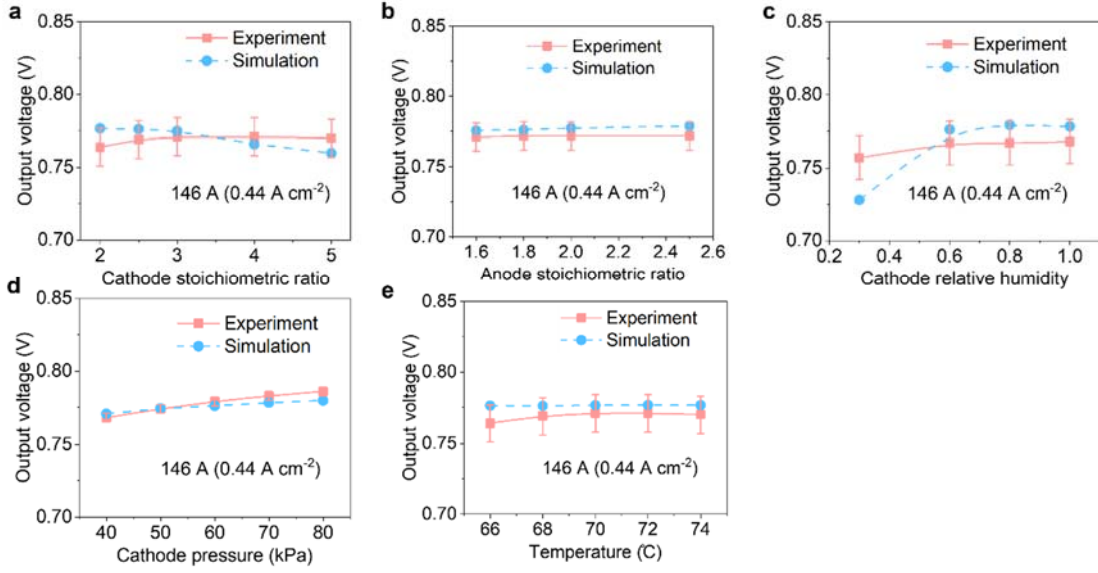


Fig. S7 Simulation performance of five sensitive parameters compared with experimental data at the current density of 146 A (0.44 A cm^{-2}).

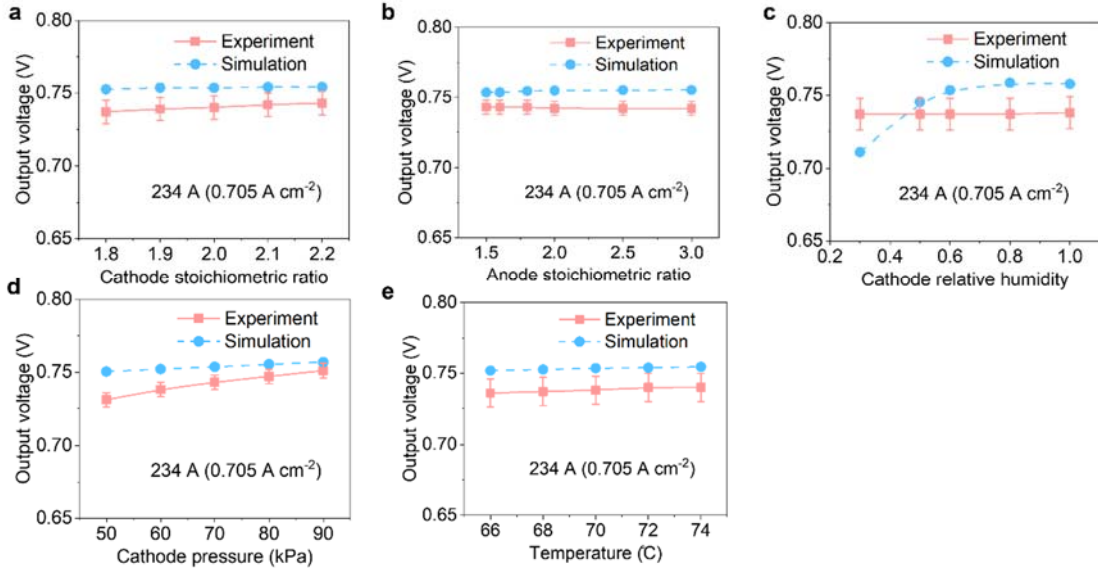


Fig. S8 Simulation performance of five sensitive parameters compared with experimental data at the current density of 234 A (0.705 A cm^{-2}).

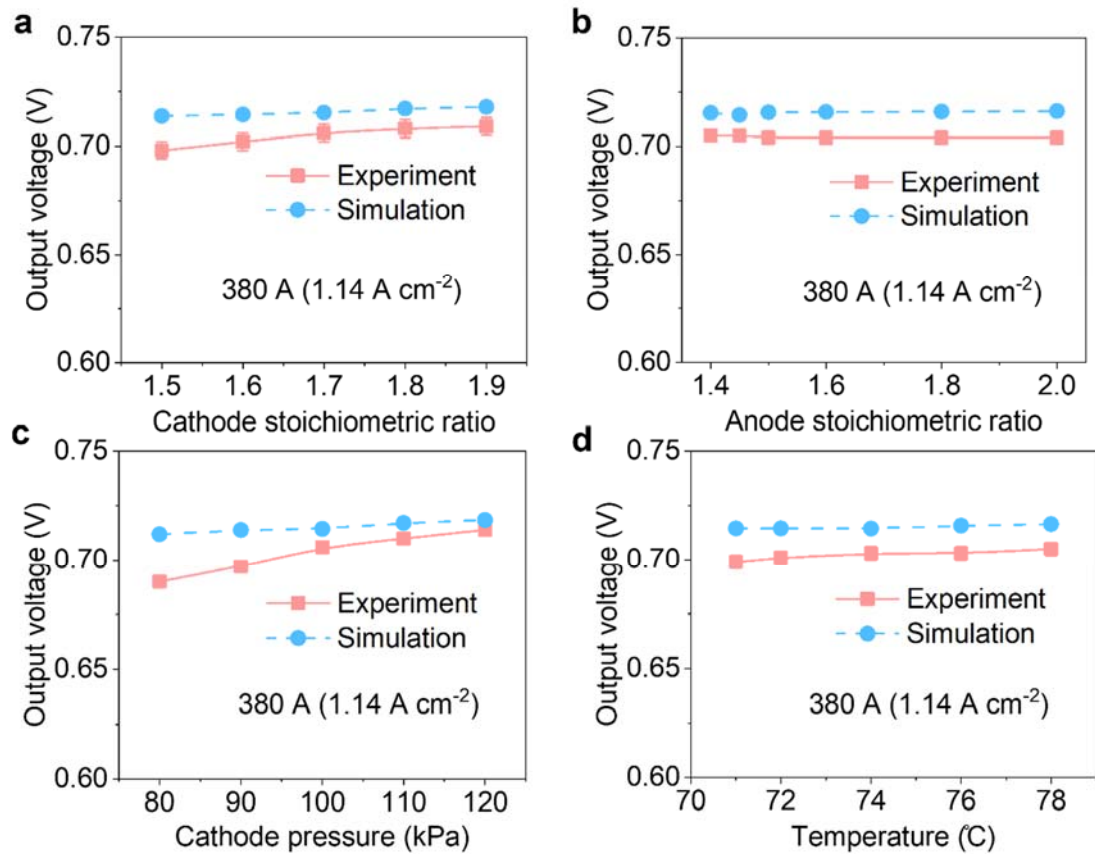


Fig. S9 Simulation performance of five sensitive parameters compared with experimental data at current densities of 380 A (1.14 A cm⁻²).

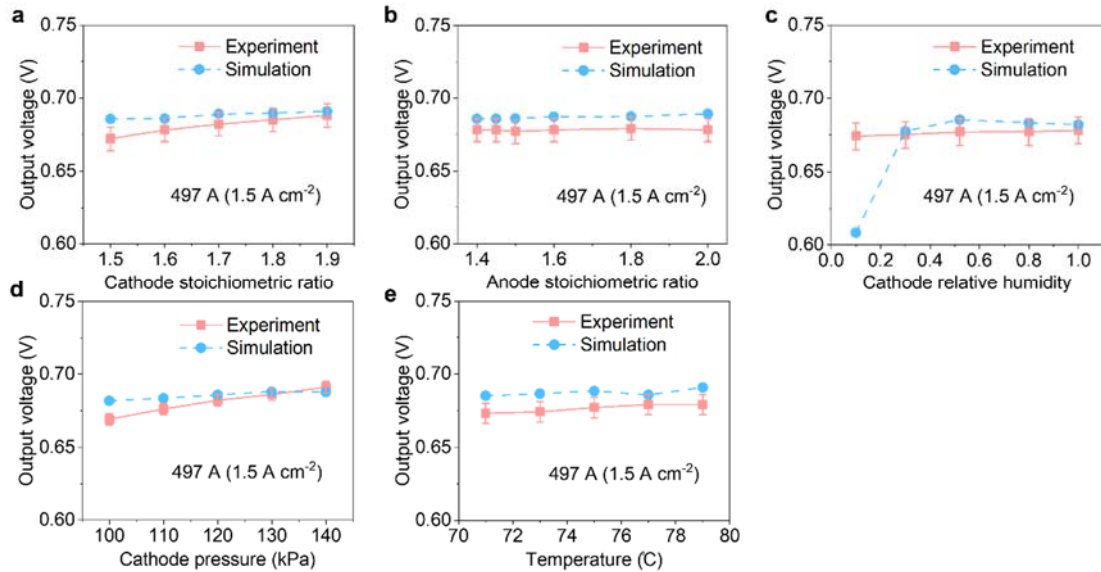


Fig. S10 Simulation performance of five sensitive parameters compared with experimental data at current densities of 497 A (1.5 A cm⁻²).

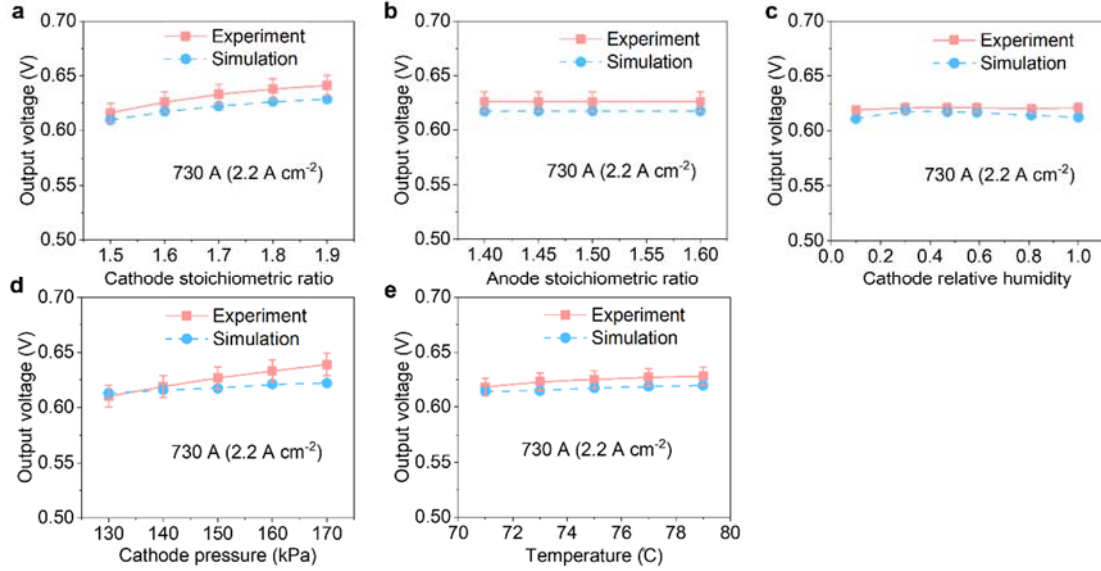


Fig. S11 Simulation performance of five sensitive parameters compared with experimental data at current densities of 730 A (2.2 A cm^{-2}).

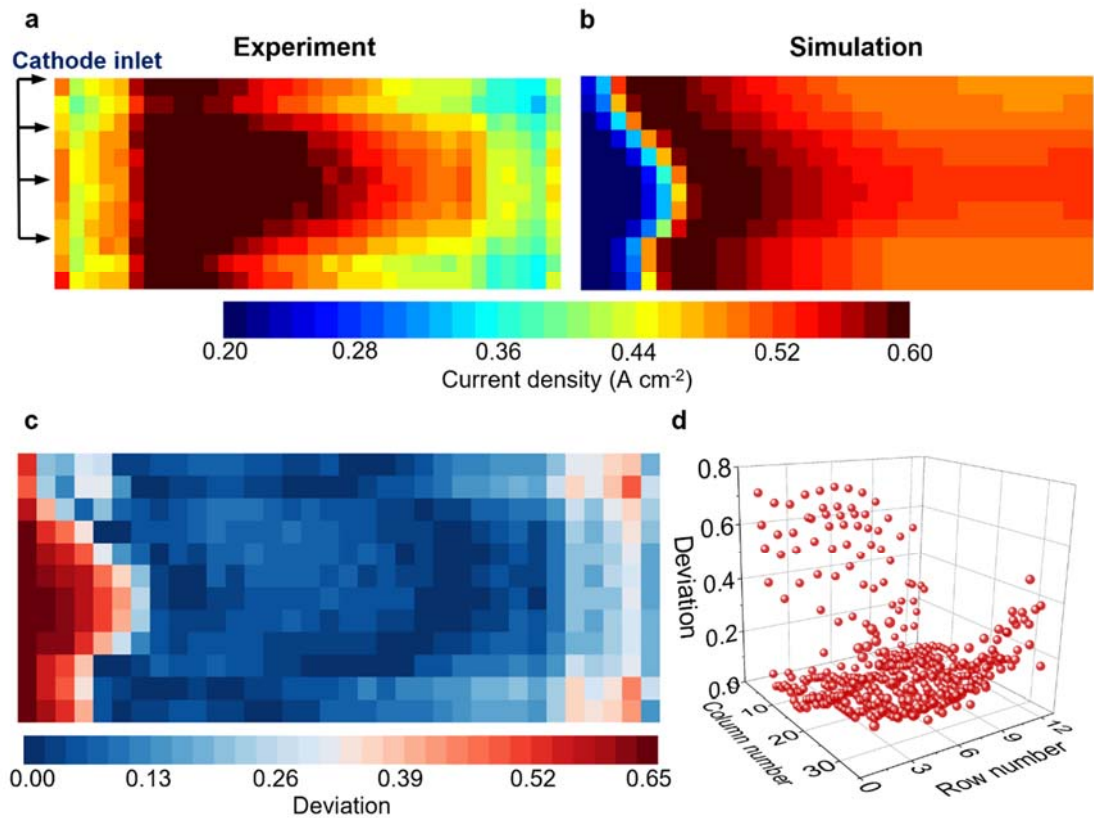


Fig. S12 Validation results and deviations at the current density of 0.5 A cm^{-2} . (a) Experimental current density distribution. (b) Simulation current density distribution. (c) Deviation distribution of 408 parts. (d) three-dimensional scatters distribution of deviations (Three coordinate axes represent deviation, column number, and row number, respectively).

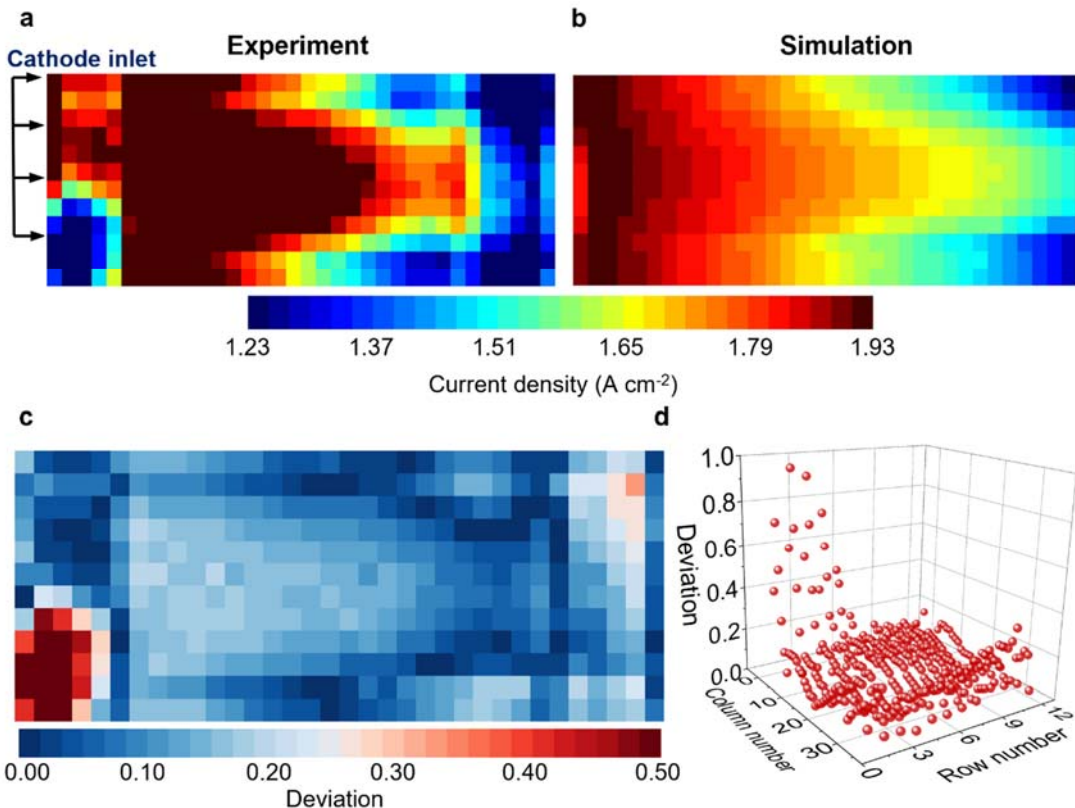


Fig. S13 Validation results and deviations at the current density of 1.7 A cm^{-2} . (a) Experimental current density distribution. (b) Simulation current density distribution. (c) Deviation distribution of 408 parts. (d) three-dimensional scatters distribution of deviations (Three coordinate axes represent deviation, column number, and row number, respectively).

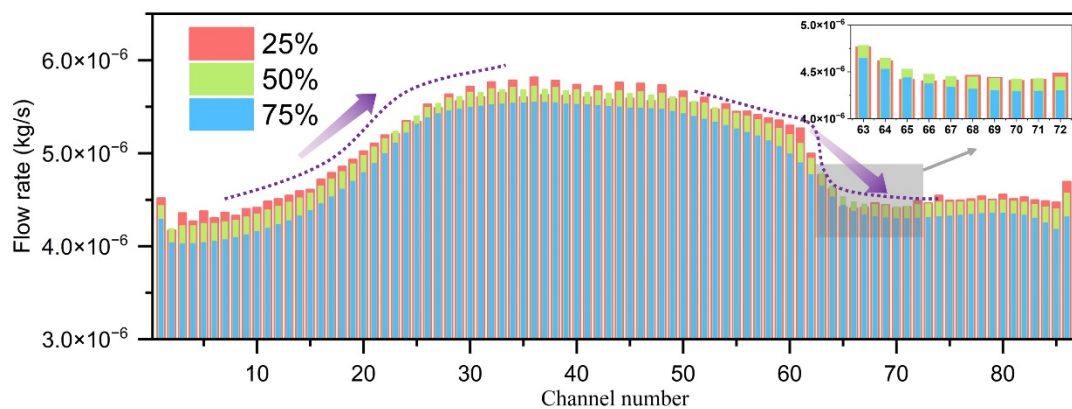


Fig. S14 Mass flow rate in each channel of cathode flow field at sections of 25%, 50% and 75% cross-sections.

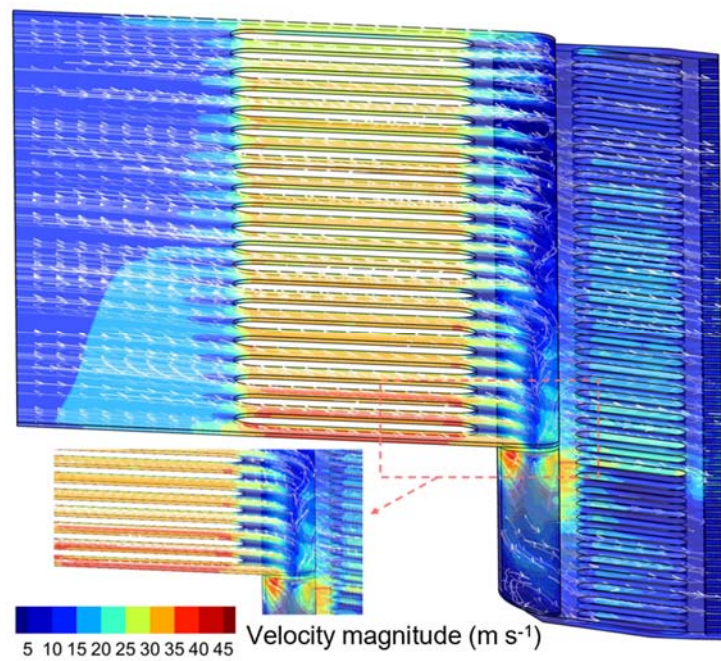


Fig. S15 Gas velocity magnitude distribution and flow streamline in cathode distribution zone and bridge-crossing zone.

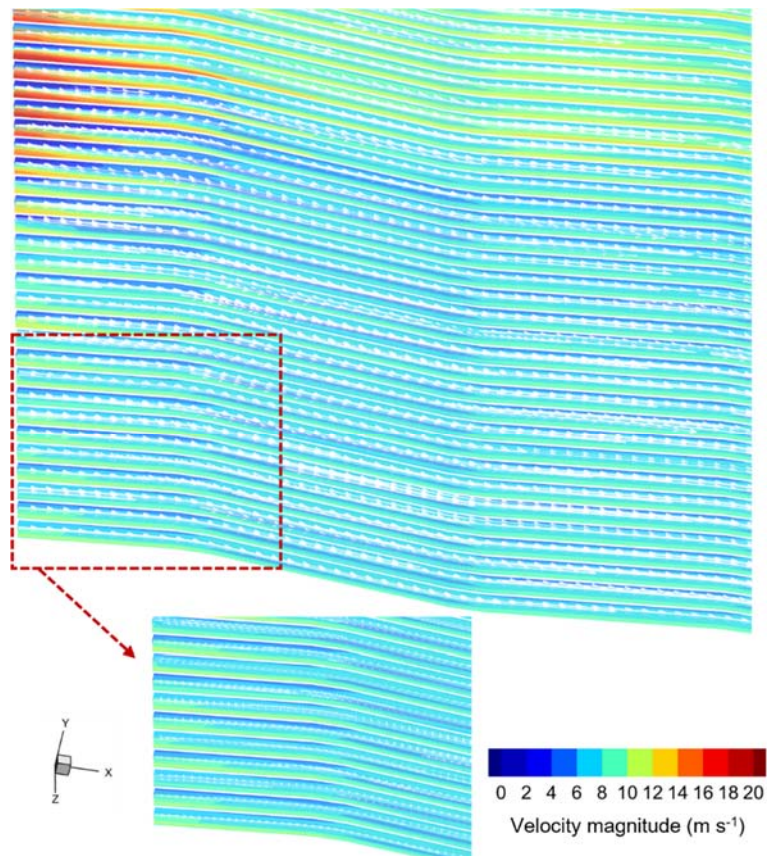


Fig. S16 Gas velocity magnitude distribution and flow streamline in cathode wavy channels.

Supplementary Tables

Table S1 Operation conditions during activation process

I (A cm ⁻²)	Time of duration (s)	RH_a	RH_c	P_a (kPa)	P_c (kPa)	ST_a	ST_c	P_{cool} (kPa)	T (°C)	ΔT (K)
0	10	50%	50%	50	40	4	7	20	65	3
0.151	120	50%	50%	50	40	4	7	20	65	3
0.265	120	50%	50%	50	40	4	2.3	20	65	5
0.44	120	50%	50%	70	60	4	2.3	50	67	5
0.705	120	50%	50%	80	70	2	2.3	50	68	7
0.88	120	50%	50%	90	80	1.8	2.3	80	70	8
1.145	120	50%	50%	110	100	1.8	2.3	80	72	8
1.319	120	50%	50%	120	110	1.8	2.0	80	74	8
1.497	120	50%	50%	130	120	1.8	2.0	80	77	9
1.638	120	50%	50%	140	130	1.8	2.0	80	77	9
1.762	120	50%	50%	150	140	1.8	2.0	80	77	10
2.0	120	50%	50%	160	150	1.6	1.6	80	77	11
2.1	120	50%	50%	160	150	1.6	1.6	80	77	11.5

Table S2 Source terms of 3D sub-model

Source terms		Units
$S_m = \begin{cases} -S_{v-l} & \text{GCHs,GDLs,MPLs} \\ -S_{v-l} + \frac{J_{vp}}{\delta_{EL}} M_{H_2O} + \frac{J_{O_2}}{\delta_{EL}} M_{O_2} & \text{CEL} \\ -S_{v-l} + \frac{J_{vp}}{\delta_{EL}} M_{H_2O} + \frac{J_{H_2}}{\delta_{EL}} M_{H_2} & \text{AEL} \end{cases}$		$\text{kg m}^{-3} \text{ s}^{-1}$
$S_u = -\frac{\mu_g}{Kk_g} \vec{u}_g$	GDLs,MPLs,ELs	$\text{kg m}^{-2} \text{ s}^{-1}$
$S_{H_2} = \frac{J_{H_2}}{\delta_{EL}} M_{H_2}$	AEL	$\text{kg m}^{-3} \text{ s}^{-1}$
$S_{O_2} = \frac{J_{O_2}}{\delta_{EL}} M_{O_2}$	CEL	$\text{kg m}^{-3} \text{ s}^{-1}$
$S_{vp} = \begin{cases} -S_{v-l} & \text{GCHs,GDLs,MPLs} \\ -S_{v-l} + \frac{J_{vp}}{\delta_{EL}} M_{H_2O} & \text{CEL} \\ -S_{v-l} + \frac{J_{vp}}{\delta_{EL}} M_{H_2O} & \text{AEL} \end{cases}$		$\text{kg m}^{-3} \text{ s}^{-1}$
$S_T = \begin{cases} hS_{v-l} + \frac{J_T}{\delta_{EL}} & \text{AEL} \\ hS_{v-l} + \frac{J_T}{\delta_{EL}} & \text{CEL} \\ hS_{v-l} + \ \nabla \phi_{ele}\ ^2 k_{ele}^{\text{eff}} & \text{GDLs,MPLs} \\ \ \nabla \phi_{ele}\ ^2 k_{ele}^{\text{eff}} & \text{BP} \\ hS_{v-l} & \text{GCHs} \end{cases}$		W m^{-3}
$S_l = \begin{cases} S_{v-l} + \frac{J_l}{\delta_{EL}} M_{H_2O} & \text{ELs} \\ S_{v-l} & \text{GDLs,MPLs} \end{cases}$		$\text{kg m}^{-3} \text{ s}^{-1}$
$S_l = S_{v-l} - \rho_l \frac{K_{\text{through}} k_l}{\mu_l \delta_{\text{mesh}}} \nabla P_l^{\text{GDL}}$	GCHs	$\text{kg m}^{-3} \text{ s}^{-1}$

$$S_{v-l} = \begin{cases} \gamma_{v-l} \epsilon (1-s)(C_{vp} - C_{sat}) M_{H_2O} & C_{vp} > C_{sat} \\ \gamma_{v-l} \epsilon s (C_{vp} - C_{sat}) M_{H_2O} & C_{vp} < C_{sat} \end{cases} \quad \text{kg m}^{-3} \text{ s}^{-1}$$

$$S_{ele} = \frac{J_{ele}}{\delta_{EL}} \quad \text{ELs} \quad \text{A m}^{-3}$$

Table S3 Source terms of 1D sub-model

Source terms	Units
$S_{H_2}^{1D} = \frac{j_a}{2F}$	kg m ⁻³ s ⁻¹ 1
$S_{O_2}^{1D} = \frac{j_c}{4F}$	kg m ⁻³ s ⁻¹ 1
$S_{vp}^{1D} = \frac{j_c}{2F} - S_{v-m}^{1D} - S_{v-l}^{1D}$	kg m ⁻³ s ⁻¹ 1
$S_{lw}^{1D} = S_{v-l}^{1D}$	kg m ⁻³ s ⁻¹ 1
$S_{v-m}^{1D} = \frac{\gamma_{v-m} (\lambda_{eq} - \lambda) \rho_{mem}}{EW}$	kg m ⁻³ s ⁻¹ 1
$S_{v-l}^{1D} = \begin{cases} \gamma_{v-l} \epsilon (1-s)(C_{vp} - C_{sat}) & C_{vp} > C_{sat} \\ \gamma_{v-l} \epsilon s (C_{vp} - C_{sat}) & C_{vp} < C_{sat} \end{cases}$	kg m ⁻³ s ⁻¹ 1
$S_{ele}^{1D} = \begin{cases} -j_a & ACL \\ j_c & CCL \end{cases}$	A m ⁻³
$S_{ion}^{1D} = \begin{cases} j_a & ACL \\ -j_c & CCL \end{cases}$	A m ⁻³

$$S_T^{1D} = \begin{cases} \frac{I^2}{k_{ele}^{CL} \varepsilon_{pt/c,ACL}^{1.5}} + \frac{I^2}{k_{ion} \varepsilon_{im,ACL}^{1.5}} + j_a (\eta_{elec,a} + \frac{T \Delta S_a}{4F}) + h S_{v-l} & ACL \\ \frac{I^2}{k_{ele}^{CL} \varepsilon_{pt/c,CCL}^{1.5}} + \frac{I^2}{k_{ion} \varepsilon_{im,CCL}^{1.5}} + j_c (\eta_{elec,c} + \frac{T \Delta S_a}{4F}) + h S_{v-l} & CCL \\ \frac{I^2}{k_{ion}} & MEM \end{cases} \quad W \text{ m}^{-3}$$

Table S4 Transport properties

Parameters	Expressions
Gas mixture density (kg m^{-3})	$\rho_g = p_g (RT \sum_i \frac{Y_i}{M_i})^{-1}$
Volume fraction of platinum/carbon catalyst	$\varepsilon_{pt/c} = \frac{m_{pt}}{\delta_{CL}} \left[\frac{1}{\rho_{pt}} + \left(\frac{1}{\zeta_{pt/c}} - 1 \right) \frac{1}{\rho_c} \right]$
Volume fraction of ionomer	$\varepsilon_{im} = \frac{\zeta_{im/c} m_{pt}}{\delta_{CL} \rho_{im}} \left(\frac{1}{\zeta_{pt/c}} - 1 \right) \left(1 + \frac{M_1 \rho_{im}}{\rho_l E W} \lambda \right)$
Porosity of CL	$\varepsilon_{CL} = 1 - \varepsilon_{pt/c} - \varepsilon_{im}$
Hydrogen diffusivity ($\text{m}^2 \text{ s}^{-1}$)	$D_{H_2} = 1.005 \times 10^{-4} \left(\frac{T}{333.15} \right)^{1.5} \left(\frac{101325}{P} \right)$
Oxygen diffusivity ($\text{m}^2 \text{ s}^{-1}$)	$D_{O_2} = 2.652 \times 10^{-4} \left(\frac{T}{333.15} \right)^{1.5} \left(\frac{101325}{P} \right)$
Water vapor diffusivity in anode components ($\text{m}^2 \text{ s}^{-1}$)	$D_{vp}^a = 1.005 \times 10^{-4} \left(\frac{T}{333.15} \right)^{1.5} \left(\frac{101325}{P} \right)$
Water vapor diffusivity in cathode components ($\text{m}^2 \text{ s}^{-1}$)	$D_{vp}^c = 1.005 \times 10^{-4} \left(\frac{T}{333.15} \right)^{1.5} \left(\frac{101325}{P} \right)$
Gas effective diffusivity ($\text{m}^2 \text{ s}^{-1}$)	$D_i^{\text{eff}} = D_i \varepsilon^{1.5} (1 - s)^{1.5}$
Dynamic viscosity of liquid	$\mu_l = 2.414 \times 10^{-5} \times 10^{247.8/(T-140.0)}$

water ($\text{kg m}^{-1} \text{ s}^{-1}$)	
Relative permeability (m^2)	$k_l = s^{3.0}, k_g = (1-s)^{3.0}$
Saturation pressure (Pa)	$\log_{10}(P_{\text{sat}} / 101325.0) = -2.1794 + 0.02953(T - 273.15) - 9.1837 \times 10^{-5}(T - 273.15)^2 + 1.4454 \times 10^{-7}(T - 273.15)^3$
Membrane water diffusivity ($\text{m}^2 \text{s}^{-1}$)	
	$D_d^{\text{eff}} = \begin{cases} 3.1 \times 10^{-7} \lambda [\exp(0.28\lambda - 1.0)] \exp(-2346.0/T) & 0 < \lambda < 3 \\ 4.17 \times 10^{-8} \lambda [161.0 \exp(-\lambda) + 1.0] \exp(-2346.0/T) & 3 \leq \lambda \geq 17 \\ 4.1 \times 10^{-10} (\lambda/25.0)^{0.15} (1.0 + \tanh((\lambda - 2.5)/1.4)) & \lambda > 17 \end{cases}$
Water Activity	$a = \frac{P_v}{P_{\text{sat}}} + 2s$
Equilibrium membrane water content	$\lambda_{\text{eq}} = \begin{cases} 0.043 + 17.81a - 39.85a^2 + 36.0a^3 & 0 \leq a \leq 1 \\ 14.0 + 14.0(a - 1.0) & 1 < a \leq 3 \end{cases}$

Table S5 Physical properties and model parameters

Parameters	Value
Pt loading (Cathode / Anode) (mgPt/cm^2)	0.42 / 0.07
I/C ratio (Cathode / Anode)	0.9 / 0.75
Pt/C mass ratio (Cathode / Anode)	0.59 / 0.37
Porosity (GDL / MPL)	0.778 / 0.5
Intrinsic permeability (GDL / MPL / CL)	$2.0 \times 10^{-12} / 1.0 \times 10^{-12} / 1.0 \times 10^{-13}$
Contact angle (GDL / MPL / CL) (°)	120 / 130 / 102
Electronic conductivity (BP / MPL / CL) (S m^{-1})	45000 / 5000 / 5000
Electronic conductivity of GDL (In-plane /)	5740.5 / 151

Through-plane) (S m ⁻¹)	
Equivalent weight of dry ionomer (g mol ⁻¹)	1020
Kinetic transfer coefficient (Cathode / Anode)	0.5 / 0.5
Condensation phase transition rate (s ⁻¹)	100
Evaporation phase transition rate (s ⁻¹)	100
Reference exchange current density (Cathode / Anode)	3.5*10 ⁻² / 3.5*10 ²
Reference hydrogen concentration (mol m ⁻³)	56.4
Reference oxygen concentration (mol m ⁻³)	3.39
Latent heat coefficient (J mol ⁻¹)	44900

Table S6 Geometry parameters

Parameters	Value
Channel width (Cathode / Anode) (mm)	0.73 / 0.54
Rib width (Cathode / Anode) (mm)	0.46 / 0.66
Channel height (Cathode / Anode) (mm)	0.28 / 0.25
GDL height (μm)	170
MPL height (μm)	25
CL height (Cathode / Anode) (μm)	7.5 / 2.5
Membrane height (μm)	8
Channel number	86

Table S7 Simulation results and experimental data of polarization curve validation

Current density (A cm^{-2})	Voltage (V) (Experiment)	Voltage (V) (Simulation)
0.1506	0.836	0.805346
0.265	0.801	0.796474
0.44	0.782	0.776185
0.70482	0.748	0.753526
0.88	0.73	0.738242
1.1446	0.706	0.714458
1.32	0.694	0.70008
1.497	0.68	0.685745
1.64	0.669	0.6732
1.76	0.661	0.662707
2.0	0.641	0.640744
2.1	0.627	0.629543
2.2	0.617	0.617296

Table S8 Experimental test conditions

<i>I</i> (A cm ⁻²)	RH _a	RH _c	P _a (kPa)	P _c (kPa)	ST _a	ST _c	T (°C)	ΔT (K)
0.1506	50%	63%	150	140	2	4	65	3
0.2651	44%	72%	150	140	1.8	2.5	67	5
0.4397	44%	60%	170	160	1.8	2.5	68	5
0.7048	38%	60%	180	170	1.6	2	70	7
0.8795	31%	60%	190	180	1.45	1.8	72	8
1.1445	31%	55%	210	200	1.45	1.6	74	8
1.3192	31%	52%	220	210	1.45	1.6	77	8
1.4969	31%	52%	230	220	1.45	1.6	77	9
1.6385	31%	49%	240	230	1.45	1.6	77	9
1.7620	31%	49%	250	240	1.45	1.6	77	10
2	31%	48%	260	250	1.45	1.6	77	11
2.0994	31%	48%	260	250	1.45	1.6	77	11.5
2.1988	31%	48%	260	250	1.45	1.6	75	12

Table S9 Experimental data of each segment in PCB testing at the current density of 0.5 A cm^{-2}

0.	0.	0.	0.	0.	0.	0.	0.	0.	0.	0.	0.	0.	0.	0.	0.	0.	0.	0.	0.	0.	0.	0.	0.	0.	0.	0.	0.
50	42	44	46	47	57	60	61	61	60	59	58	57	56	54	53	53	51	50	49	48	47	45	44	44	43	43	41
0.	0.	0.	0.	0.	0.	0.	0.	0.	0.	0.	0.	0.	0.	0.	0.	0.	0.	0.	0.	0.	0.	0.	0.	0.	0.	0.	0.
45	39	43	45	46	52	59	59	59	59	58	58	56	55	54	52	52	50	49	48	47	46	46	43	43	42	42	39
0.	0.	0.	0.	0.	0.	0.	0.	0.	0.	0.	0.	0.	0.	0.	0.	0.	0.	0.	0.	0.	0.	0.	0.	0.	0.	0.	0.
47	42	43	46	49	56	63	61	62	62	63	62	61	59	57	57	56	55	54	52	52	50	49	48	47	46	46	44
0.	0.	0.	0.	0.	0.	0.	0.	0.	0.	0.	0.	0.	0.	0.	0.	0.	0.	0.	0.	0.	0.	0.	0.	0.	0.	0.	0.
47	43	46	48	48	58	64	64	63	64	64	63	62	61	61	59	59	57	56	55	54	53	52	50	49	48	47	49
0.	0.	0.	0.	0.	0.	0.	0.	0.	0.	0.	0.	0.	0.	0.	0.	0.	0.	0.	0.	0.	0.	0.	0.	0.	0.	0.	0.
50	44	46	48	50	56	62	61	63	62	64	63	63	61	61	60	58	58	56	54	54	53	52	51	50	49	50	47
0.	0.	0.	0.	0.	0.	0.	0.	0.	0.	0.	0.	0.	0.	0.	0.	0.	0.	0.	0.	0.	0.	0.	0.	0.	0.	0.	0.
50	44	47	49	49	56	62	62	60	61	64	61	62	63	61	61	59	59	56	58	56	55	53	52	51	50	51	48
0.	0.	0.	0.	0.	0.	0.	0.	0.	0.	0.	0.	0.	0.	0.	0.	0.	0.	0.	0.	0.	0.	0.	0.	0.	0.	0.	0.
50	44	45	48	49	56	61	60	61	61	61	62	61	62	61	60	60	59	58	57	56	54	54	53	52	50	50	51
0.	0.	0.	0.	0.	0.	0.	0.	0.	0.	0.	0.	0.	0.	0.	0.	0.	0.	0.	0.	0.	0.	0.	0.	0.	0.	0.	0.
49	44	46	48	50	55	63	62	62	61	62	62	61	60	61	59	58	59	57	56	55	53	52	52	50	50	49	50
0.	0.	0.	0.	0.	0.	0.	0.	0.	0.	0.	0.	0.	0.	0.	0.	0.	0.	0.	0.	0.	0.	0.	0.	0.	0.	0.	0.
48	43	47	48	50	57	62	62	62	62	61	60	59	57	58	57	56	55	54	52	52	50	49	48	47	47	48	45
0.	0.	0.	0.	0.	0.	0.	0.	0.	0.	0.	0.	0.	0.	0.	0.	0.	0.	0.	0.	0.	0.	0.	0.	0.	0.	0.	0.
48	43	46	50	48	58	61	64	62	62	61	60	59	56	55	54	54	52	51	51	50	48	47	46	46	45	45	43
0.	0.	0.	0.	0.	0.	0.	0.	0.	0.	0.	0.	0.	0.	0.	0.	0.	0.	0.	0.	0.	0.	0.	0.	0.	0.	0.	0.
49	42	45	45	46	56	60	59	60	60	57	56	54	53	52	50	50	48	46	47	45	45	44	43	42	41	43	40
0.	0.	0.	0.	0.	0.	0.	0.	0.	0.	0.	0.	0.	0.	0.	0.	0.	0.	0.	0.	0.	0.	0.	0.	0.	0.	0.	0.
54	45	45	47	48	56	61	61	62	61	60	58	56	54	53	52	50	50	49	48	47	46	46	45	44	43	43	40

Table S10 Experimental data of each segment in PCB testing at the current density of 1.5 A cm^{-2}

1.	1.	1.	1.	1.	1.	1.	1.	1.	1.	1.	1.	1.	1.	1.	1.	1.	1.	1.	1.	1.	1.	1.	1.	1.	1.	1.	1.		
97	59	61	61	57	83	90	89	85	81	76	71	66	59	54	52	51	46	45	43	38	33	26	23	21	21	24	31		
1.	1.	1.	1.	1.	1.	1.	1.	1.	1.	1.	1.	1.	1.	1.	1.	1.	1.	1.	1.	1.	1.	1.	1.	1.	1.	1.	1.	1.	
79	50	54	55	53	68	84	80	78	74	70	65	58	56	51	46	46	43	40	37	34	28	25	18	16	15	18	25	18	
1.	1.	1.	1.	1.	1.	1.	1.	1.	1.	1.	1.	1.	1.	1.	1.	1.	1.	1.	1.	1.	1.	1.	1.	1.	1.	1.	1.	1.	1.
86	60	59	60	63	81	97	87	86	83	83	77	73	66	61	61	57	57	57	50	47	42	35	31	26	24	28	35	33	
1.	1.	1.	1.	1.	1.	1.	2.	1.	1.	1.	1.	1.	1.	1.	1.	1.	1.	1.	1.	1.	1.	1.	1.	1.	1.	1.	1.	1.	1.
85	62	64	67	63	89	02	99	95	91	89	84	80	77	75	70	69	66	64	60	56	53	47	42	37	34	34	46	42	
1.	1.	1.	1.	1.	1.	1.	2.	1.	1.	1.	1.	1.	1.	1.	1.	1.	1.	1.	1.	1.	1.	1.	1.	1.	1.	1.	1.	1.	1.
84	60	63	67	69	83	01	96	98	92	93	90	89	81	80	78	75	73	72	67	61	60	54	50	46	43	51	45	31	
1.	1.	1.	1.	1.	1.	1.	2.	2.	1.	1.	1.	1.	1.	1.	1.	1.	1.	1.	1.	1.	1.	1.	1.	1.	1.	1.	1.	1.	1.
72	54	61	66	65	88	03	02	95	93	99	89	90	89	84	82	76	76	69	72	66	63	56	53	48	45	50	55	48	
1.	1.	1.	1.	1.	1.	1.	2.	1.	1.	1.	1.	1.	1.	1.	1.	1.	1.	1.	1.	1.	1.	1.	1.	1.	1.	1.	1.	1.	1.
66	46	52	62	65	87	01	96	97	95	93	92	89	87	83	80	80	75	74	70	67	61	58	54	50	46	47	56	47	
1.	1.	1.	1.	1.	1.	1.	2.	1.	1.	1.	1.	1.	1.	1.	1.	1.	1.	1.	1.	1.	1.	1.	1.	1.	1.	1.	1.	1.	1.
49	33	44	57	62	82	04	99	97	94	93	90	87	84	83	77	73	74	70	66	62	56	52	48	43	42	41	49	45	
1.	1.	1.	1.	1.	1.	1.	1.	1.	1.	1.	1.	1.	1.	1.	1.	1.	1.	1.	1.	1.	1.	1.	1.	1.	1.	1.	1.	1.	1.
33	19	38	50	57	82	98	95	91	92	89	83	81	76	70	70	67	62	62	58	51	49	43	39	36	32	34	40	36	
1.	1.	1.	1.	1.	1.	1.	1.	1.	1.	1.	1.	1.	1.	1.	1.	1.	1.	1.	1.	1.	1.	1.	1.	1.	1.	1.	1.	1.	1.
27	15	33	51	52	80	90	95	86	83	80	75	71	64	62	57	54	49	46	44	41	34	32	27	25	22	21	27	27	
1.	1.	1.	1.	1.	1.	1.	1.	1.	1.	1.	1.	1.	1.	1.	1.	1.	1.	1.	1.	1.	1.	1.	1.	1.	1.	1.	1.	1.	1.
28	18	36	43	48	75	86	80	77	75	67	62	57	53	49	44	40	36	29	31	25	22	18	17	11	10	08	17	15	
1.	1.	1.	1.	1.	1.	1.	1.	1.	1.	1.	1.	1.	1.	1.	1.	1.	1.	1.	1.	1.	1.	1.	1.	1.	1.	1.	1.	1.	1.
48	32	44	53	55	79	93	89	86	82	75	70	62	55	50	47	39	35	33	28	26	23	19	15	13	12	13	20	16	

Table S11 Experimental data of each segment in PCB testing at the current density of 1.7 A cm⁻²

2. 28	1. 84	1. 85	1. 84	1. 80	2. 07	2. 15	2. 14	2. 10	2. 06	2. 00	1. 95	1. 91	1. 84	1. 79	1. 77	1. 76	1. 70	1. 67	1. 65	1. 59	1. 54	1. 45	1. 41	1. 40	1. 41	1. 45	1. 49	1. 38	1. 21	1. 17	1. 10	1. 07	1. 27
2. 08	1. 73	1. 77	1. 77	1. 74	1. 91	1. 08	1. 03	1. 01	1. 97	1. 93	1. 89	1. 82	1. 81	1. 76	1. 71	1. 71	1. 66	1. 62	1. 59	1. 56	1. 49	1. 45	1. 37	1. 35	1. 38	1. 42	1. 45	1. 30	1. 16	1. 14	1. 07	1. 99	1. 18
2. 16	1. 86	1. 83	1. 83	1. 86	1. 06	1. 23	1. 12	1. 11	1. 07	1. 08	1. 02	1. 99	1. 92	1. 88	1. 88	1. 83	1. 82	1. 81	1. 74	1. 71	1. 65	1. 58	1. 54	1. 49	1. 50	1. 56	1. 58	1. 48	1. 26	1. 25	1. 14	1. 11	1. 26
2. 17	1. 89	1. 90	1. 92	1. 86	1. 15	1. 29	1. 25	1. 20	1. 17	1. 14	1. 09	1. 06	1. 03	1. 02	1. 96	1. 96	1. 92	1. 89	1. 86	1. 82	1. 79	1. 74	1. 68	1. 63	1. 63	1. 72	1. 59	1. 36	1. 33	1. 24	1. 18	1. 33	
2. 18	1. 86	1. 89	1. 91	1. 92	1. 08	1. 28	1. 22	1. 24	1. 18	1. 19	1. 15	1. 14	1. 06	1. 06	1. 05	1. 01	1. 98	1. 98	1. 93	1. 87	1. 87	1. 81	1. 78	1. 74	1. 72	1. 72	1. 77	1. 64	1. 44	1. 37	1. 32	1. 25	1. 44
2. 01	1. 77	1. 83	1. 87	1. 86	1. 12	1. 30	1. 29	1. 20	1. 19	1. 25	1. 13	1. 14	1. 13	1. 09	1. 08	1. 02	1. 02	1. 95	1. 98	1. 93	1. 91	1. 83	1. 81	1. 76	1. 75	1. 80	1. 80	1. 66	1. 45	1. 44	1. 33	1. 29	1. 45
1. 83	1. 56	1. 61	1. 72	1. 78	1. 06	1. 25	1. 20	1. 22	1. 21	1. 18	1. 18	1. 14	1. 13	1. 08	1. 07	1. 07	1. 02	1. 01	1. 98	1. 95	1. 88	1. 86	1. 82	1. 79	1. 76	1. 78	1. 83	1. 67	1. 45	1. 42	1. 38	1. 27	1. 46
1. 55	1. 30	1. 36	1. 49	1. 62	1. 92	1. 22	1. 21	1. 22	1. 21	1. 20	1. 17	1. 14	1. 10	1. 10	1. 04	1. 00	1. 03	1. 99	1. 95	1. 92	1. 85	1. 82	1. 78	1. 74	1. 74	1. 79	1. 68	1. 47	1. 45	1. 35	1. 29	1. 43	
1. 34	1. 09	1. 20	1. 31	1. 48	1. 90	1. 18	1. 19	1. 18	1. 20	1. 17	1. 11	1. 10	1. 04	1. 98	1. 99	1. 96	1. 91	1. 91	1. 86	1. 80	1. 78	1. 72	1. 67	1. 63	1. 60	1. 64	1. 71	1. 58	1. 45	1. 41	1. 31	1. 25	1. 40
1. 22	1. 00	1. 12	1. 35	1. 50	1. 96	1. 16	1. 24	1. 15	1. 12	1. 09	1. 03	1. 99	1. 92	1. 90	1. 85	1. 83	1. 76	1. 72	1. 70	1. 67	1. 59	1. 56	1. 50	1. 47	1. 45	1. 45	1. 53	1. 48	1. 30	1. 31	1. 24	1. 18	1. 33
1. 18	0. 98	1. 12	1. 33	1. 53	1. 94	1. 14	1. 08	1. 05	1. 03	1. 94	1. 89	1. 84	1. 81	1. 76	1. 71	1. 67	1. 61	1. 53	1. 55	1. 47	1. 43	1. 39	1. 36	1. 30	1. 29	1. 27	1. 38	1. 33	1. 21	1. 23	1. 16	1. 09	1. 26
1. 35	1. 11	1. 25	1. 47	1. 64	1. 99	1. 21	1. 18	1. 16	1. 12	1. 04	1. 99	1. 90	1. 83	1. 78	1. 76	1. 66	1. 61	1. 58	1. 52	1. 49	1. 44	1. 40	1. 35	1. 31	1. 31	1. 32	1. 40	1. 33	1. 23	1. 24	1. 18	1. 13	1. 41

Table S12 Pressure drops across different sections

Zone	Pressure drop (kPa)
Inlet (IN) - Bridge-crossing zone (BCI)	4.37
Bridge-crossing in (BCI) - Distribution in (DI)	0.46
Distribution in (DI) - Distribution out (DO)	10.13
Distribution out (DO) – Bridge-crossing out (BCO)	0.93
Bridge-crossing out (BCO) – Outlet (OUT)	10.12
Inlet (IN) – Outlet (OUT)	26.01

Supplementary Notes

Note S1. Suggestions for standards when conducting this method

When using this method and conducting the procedure, some standards are suggested based on this study:

1. For the first time, we have clarified the geometric simplification standard for the 3D PEM fuel cell model. Certain fine structures, like sharp angles and chamfers, can be simplified as required; otherwise, mesh generation will become more difficult and has little influence on performance. Nevertheless, the details of concerned structures, such as bridge-crossing zones, distribution zones, and channels, should be retained. The overall outlines of these structures should also be maintained. For example, different types of channels, such as wavy, straight, baffled, and partial-narrow ones, should be distinguishable.
2. For the first time, we have clarified the construction standard for the 3D PEM fuel cell model. In large-scale simulations, numerous equations, mechanisms, and parameters need to be considered. To enhance the computational efficiency while simultaneously ensuring the accuracy of the model, certain equations can be simplified. These include the membrane water content conservation equation, the ion potential conservation equation, and the liquid pressure conservation equation solved in the microporous layers and catalyst layers. Some mechanisms can be disregarded, such as nitrogen permeation across membranes and parasitic currents. When the precision requirement is not overly high, the gas-liquid two-phase flow in gas channels can sometimes be simplified to a mist state. Consequently, the liquid water saturation equation can be simplified, thereby reducing the difficulty of solving. Nevertheless, some equations must be considered, including the mass, momentum, energy, electron potential, and species conservation equations. It is recommended to use the Butler-Volmer equation rather than the Tafel equation, and to consider the aggregation correction for a detailed micro transport process in catalyst layers.

3. For the first time, we have clarified the standard for validating the 3D PEM fuel cell model. To meet the minimum requirement for ensuring model accuracy, at least two polarization curves under different operating conditions or one polarization curve along with high frequency resistance for ohmic loss testing are required. To further enhance the accuracy of model validation, sensitive parameters such as temperature, relative humidity, stoichiometric ratio, and pressure under different current densities and spatial distributions are recommended. It is preferable to conduct the model validation using a PEM fuel cell of the same size as that in the experiment. However, if this is too difficult to accomplish, it is also acceptable to use single channels extracted from the entire fuel cell, provided that their length, width, height, and shape are consistent.
4. For the first time, we have proposed a digital method to assist the structure design of PEM fuel cells, which includes backward engineering and forward design. Backward engineering requires a comprehensive process of digitalizing the original structure into mathematical geometries and meshes, developing an accurate mechanism model, and validating this model. Each step should conform to the standards provided above. Forward design is a general approach applicable to any PEM fuel cell structure design. Based on the validated model obtained from backward engineering, the defects in the original structure should be analyzed in terms of performance, losses, flow trajectory, and distributions of key parameters, etc. Subsequently, optimized structures should be proposed to address these problems and meet the expected objectives. For example, in this study, by using this method, we optimized the distribution zones, and as a result, the maximum deviation of oxygen concentration in the channels decreases from 26.33% to 3.78%.
5. For the first time, we have presented a comprehensive set of experimental data for a commercial-sized PEM fuel cell. In this study, one polarization curve, five sensitive parameters under seven current densities (ranging from low to high), and high-resolution spatial distributions under three current densities have been tested. Detailed data, especially the current density in each segment, are available.

Additionally, the experimental metallic bipolar plate and its geometry with detailed parameters are also provided. According to standard 3, other researchers can utilize our experimental data to carry out comprehensive validations for their models.

Note S2. The method of distinguishing three types of losses

The expressions of the Butler-Volmer equation considering agglomerate correction are listed below:

$$j_a = i_{0,a}^{\text{ref}} A_{\text{pt}}^{\text{eff}} \theta_{T,a} \left(\frac{RT C_{H_2}}{H_{H_2} C_{H_2}^{\text{ref}}} \right)^{0.5} \left[\exp\left(\frac{2F\alpha_a \eta_a}{RT}\right) - \exp\left(-\frac{2F(1-\alpha_a)\eta_a}{RT}\right) \right] \quad (1)$$

$$j_c = \frac{RTC_{O_2}}{H_{O_2}} \left[\frac{C_{O_2}^{\text{ref}}}{i_{0,c}^{\text{ref}} A_{\text{pt}}^{\text{eff}} \theta_{T,c} \left[\exp\left(\frac{4F\alpha_c \eta_c}{RT}\right) - \exp\left(-\frac{4F(1-\alpha_c)\eta_c}{RT}\right) \right]} + \frac{R_{\text{local}}}{4FA_{\text{im}}} \right]^{-1} \quad (2)$$

After calculating these two equations, we can obtain the anode and cathode overpotential loss caused by electrochemical reaction, η_a and η_c . The loss is the total of activation loss and concentration loss.

Then we can use the inlet hydrogen and oxygen concentrations to replace the concentrations in equation (1) and (2), respectively to calculate activation losses.¹ The modified equations are listed below:

$$j_a = i_{0,a}^{\text{ref}} A_{\text{pt}}^{\text{eff}} \theta_{T,a} \left(\frac{RT C_{H_2}^{\text{inlet}}}{H_{H_2} C_{H_2}^{\text{ref}}} \right)^{0.5} \left[\exp\left(\frac{2F\alpha_a \eta_a}{RT}\right) - \exp\left(-\frac{2F(1-\alpha_a)\eta_a}{RT}\right) \right] \quad (3)$$

$$j_c = \frac{RTC_{O_2}^{\text{inlet}}}{H_{O_2}} \left[\frac{C_{O_2}^{\text{ref}}}{i_{0,c}^{\text{ref}} A_{\text{pt}}^{\text{eff}} \theta_{T,c} \left[\exp\left(\frac{4F\alpha_c \eta_c}{RT}\right) - \exp\left(-\frac{4F(1-\alpha_c)\eta_c}{RT}\right) \right]} + \frac{R_{\text{local}}}{4FA_{\text{im}}} \right]^{-1} \quad (4)$$

After calculating equation (3) and (4), we can obtain the anode activation loss and cathode activation loss due to neglecting mass transfer and loss, $\eta_a^{\text{activation}}$ and $\eta_c^{\text{activation}}$.

Therefore, the concentration loss can be calculated by subtracting the activation loss from the overpotential loss:

$$\eta_a^{\text{concentration}} = \eta_a - \eta_a^{\text{activation}} \quad (5)$$

$$\eta_c^{\text{concentration}} = \eta_c - \eta_c^{\text{activation}} \quad (6)$$

The anode electric ohmic loss is calculated by the difference of electric potential in anode BP and electric potential in anode CL, and the cathode electric ohmic loss is calculated by the difference of electric potential in cathode CL and electric potential in cathode BP. The ionic ohmic loss is calculated by the difference of ionic potential in anode CL and cathode CL.² The expression is listed below:

$$\eta_{\text{ohmic}} = (\phi_{\text{ele}}^{\text{ABP}} - \phi_{\text{ele}}^{\text{ACL}}) + (\phi_{\text{ion}}^{\text{ACL}} - \phi_{\text{ion}}^{\text{CCL}}) + (\phi_{\text{ele}}^{\text{CCL}} - \phi_{\text{ele}}^{\text{CBP}}) \quad (7)$$

Note S3. Nomenclature

A	Specific surface area (m^{-1})
C	Molar concentration
C_p	Specific heat capacity ($\text{J mol}^{-1} \text{K}^{-1}$)
D_{eff}	Effective gas diffusivity ($\text{m}^2 \text{s}^{-1}$)
D_l	Liquid water diffusivity ($\text{m}^2 \text{s}^{-1}$)
EW	Equivalent weight (kg mol^{-1})
F	Faraday constant
H	Henry's constant ($\text{Pa m}^3 \text{mol}^{-1}$)
i_0^{ref}	Reference exchange current density (A m^{-2})
K	Intrinsic permeability (m^2)
k	Relative permeability, conductivity ($\text{m}^3, \text{W m}^{-1} \text{K}^{-1}$)
P	Pressure (Pa)
R	Universal gas constant ($\text{J mol}^{-1} \text{K}^{-1}$), resistance ($\text{m} \Omega \text{cm}^2$)
R_{local}	Local transport resistance (s m^{-1})
S	Source term ($\text{kg m}^{-3} \text{s}^{-1}, \text{kg m}^{-2} \text{s}^{-1}, \text{W m}^{-3}$), entropy change ($\text{J mol}^{-1} \text{K}^{-1}$)
s	Liquid water saturation
T	Temperature (K)
u	Velocity (m s^{-1})
Y	Gas species mass fraction

Abbreviations

1D	One-dimensional
----	-----------------

3D	Three-dimensional
BP	Bipolar plate
CL	Catalyst layer
CT	Computational tomography
CV	Cyclic voltammetry
EIS	Electrochemical impedance spectroscopy
EL	Extra layer
GCH	Gas channel
GDL	Gas diffusion layer
MEA	Membrane electrode assembly
MPL	Micro porous layer
PCB	Printed circuit board
PEM	Proton exchange membrane

Greek letters

α	Transfer coefficient
δ	Thickness (m)
η	Overpotential (V)
θ	Correction coefficient
λ	Membrane water content
μ	Dynamic viscosity ($\text{kg m}^{-1} \text{ s}^{-1}$)
ρ	Density ($\text{kg m}^{-1} \text{ s}^{-1}$)
ϕ	Potential (V)

Subscripts and superscripts

a	Anode
c	Cathode, capillary force, compressed
eff	Effective
ele	Electronic
g	Gas mixture
H ₂	Hydrogen
i	Gas species
im	Ionomer
ion	Ionic
l	Liquid water
m	Mass
mix	Mixture
mw	Membrane water
n	node
O ₂	Oxygen
pt	Platinum
ref	Reference
T	Temperature

Supplementary Reference

1. B. Liu, W. Huo, B. Xie, Q. Gao, Z. Bao, H. Li, K. Wu, S. He, Q. Du, B. Qin and K. Jiao, *Int. J. Heat Mass Transf.*, 2024, **222**, 125169.
2. K. Jiao and X. Li, *Prog. Energy Combust. Sci.*, 2011, **37**, 221-291.